

Novel Copper(II) Induced Formation of a Porphyrinogen Derivative: X-ray Structural, Spectroscopic, and Electrochemical Studies of Porphyrinogen Complexes of Cu(II) and Co(III) Complex of a Trispyrazolyl Tripodal Ligand

Sachindranath Paul,[†] Anil Kumar Barik,[‡] Shie Ming Peng,[§] and Susanta Kumar Kar^{*||}

Department of Chemistry, SreeChaitanya College, Habra, North 24 Parganas, West Bengal, India, Department of Chemistry, St. Paul's C.M. College, 33/1, Raja Rammohan Roy Sarani, Calcutta 700 009, India, Department of Chemistry, National Taiwan University, Taipei, Taiwan, 106 Republic of China, and Department of Chemistry, University College of Science, 92 A.P.C. Road, Calcutta 700 009, India

Received November 29, 2001

Copper(II) complexes of a novel pyrazole containing porphyrinogen and cobalt(III) and zinc(II) complexes of a pyrazole containing tripodal ligand having N-donor atoms have been investigated. 5-Methyl-3-formylpyrazole (MPA) on reaction with copper(II) nitrate or perchlorate in the presence of tris(2-aminoethyl)amine (tren) forms novel pyrazole-based porphyrinogen complexes [Cu(T₃-porphyrinogen)(H₂O)](NO₃)₂ (**1a**) and [Cu(T₃-porphyrinogen)(H₂O)]-(ClO₄)₂ (**1b**) where T₃-porphyrinogen is 1,6,11,16-tetraaza-5,10,15,20-tetrahydroxy-2,7,12,17-tetramethylporphyrinogen. The same products are also obtained when tren is replaced by triethylamine. By contrast, the reaction between MPA, tren, and cobalt(II) perchlorate produces the cobalt(III) complex [Co(HMPz₃tren)]ClO₄ (**2**) derived from the tripodal Schiff base tris[4-(3-(5-methyl-pyrazolyl)-3-aza-3-butenyl)amine (H₃MPz₃tren). The X-ray crystal structures of the copper(II) complexes (**1a** and **1b**) and the cobalt(III) complex (**2**) have been determined. The structures show distorted square pyramidal coordination environments for **1a** and **1b** with the water molecule occupying the apical site, while for complex **2** a distorted octahedral geometry is obtained. Data for **1a** follow: *a* = 19.476(3) Å, *b* = 9.4116(8) Å, *c* = 14.204(3) Å; α = 90° = γ, β = 107.58(2)°; *V* = 2482.0(7) Å³, *Z* = 4. Data for **1b** follow: *a* = 20.967(3) Å, *b* = 9.1563(18) Å, *c* = 14.858(4) Å; α = 90° = γ, β = 108.44(3)°; *V* = 2706.0(10) Å³, *Z* = 4. Data for **2** follow: *a* = 21.293(3) Å, *b* = 12.724(2) Å, *c* = 19.777(4) Å; α = 90° = γ, β = 93.03(2)°; *V* = 5350.6(15) Å³, *Z* = 8. All three complexes crystallize in the monoclinic crystal system with the *C2/c* space group. The complexes are further characterized by UV-vis, IR, EPR, and electrochemical studies.

Introduction

Metal complexes of chiral porphyrins, inverted porphyrins, porphyrin oligomers, and metalloporphyrins are of great current interest because of their relevance to asymmetric synthesis, chiral recognition, stabilization of unusual oxidation states, and the mechanism of photosynthesis.^{1–5} Porphyrinogen is the chemical and biochemical precursor of porphyrins.⁶ Bonomo et al. in a recent study have reported the genesis of porphodimethene, the skeleton paving the way

from porphyrinogen to porphyrin.⁷ Several recent studies have focused on the development of core-modified porphyrins and their metalation.^{1–8} Moreover, large numbers of

* To whom correspondence should be addressed. E-mail: skkar@mail.cucc.ernet.in.

[†] SreeChaitanya College.

[‡] St. Paul's C.M. College.

[§] National Taiwan University.

^{||} University College of Science.

- (1) Latos-Grazynski, L. Core Modified Heteroanalogues of Porphyrins and Metalloporphyrins. In *The Porphyrin Handbook*; Kadish, K. M., Smith, K. M., Guillard, R., Eds.; Academic Press: New York, 2000; Vol. 2, p 361.
- (2) Mazzanti, M.; Marchon, J.-C.; Wojaczynski, J.; Wolowiec, S.; Latos-Grazynski, L.; Shang, M.; Scheidt, W. R. *Inorg. Chem.* **1998**, *37*, 2476–2481.
- (3) Chmielewski, P. J.; Latos-Grazynski, L.; Schmidt, I. *Inorg. Chem.* **2000**, *39*, 5475–5482 and references therein.
- (4) Wojaczynski, J.; Latos-Grazynski, L.; Chmielewski, P. J.; Calcar, P. V.; Balch, A. L. *Inorg. Chem.* **1999**, *38*, 3040–3050.
- (5) (a) Floriani, C.; Floriani-Moro, R. In *The Porphyrin Handbook*; Kadish, K. M., Smith, K. M., Guillard, R., Eds.; Academic: Burlington, MA, 1999; Vol. 3, Chapter 25 and references therein. (b) Bonomo, L.; Solari, E.; Floriani, C.; Chiesi-villa, A.; Rizzoli, C. *J. Am. Chem. Soc.* **1998**, *120*, 12972.

metalloproteins are involved in different biological electron-transfer reactions as well as in redox processes involving molecular oxygen where the Cu(II) ion is found in active sites.^{9–15} The coordination chemistry of tripodal ligands has received considerable attention in recent years because of the diversity of physicochemical and structural features displayed by their metal complexes.^{16–21} Some of these ligands have been used to mimic the active sites of several metalloproteins. For example, copper complexes of sterically demanding tris(pyrazolyl) hydroborate ligands have found application as synthetic analogues for cuproprotein active sites.²² Hemocyanine (HC),^{13,23} the most effective model to date for the dioxygen transport protein, utilizes the ligand tris[1,3,5-diisopropylpyrazole] hydroborate.

Attempts have been made to prepare Cu(II), Co(III), and Zn(II) complexes of the tripodal ligand H₃MPz₃tren by the reaction of tren and MPA²⁴ in 1:3 molar proportion and corresponding metal salts in ethanol solution using template methodology. In the case of Cu complexes, we have a novel observation. The Cu(II) ion induced macrocyclic complexes are isolated instead of those with the desired tripodal ligand. Thus, tren acts as a base in Cu(II) ion induced macrocycle

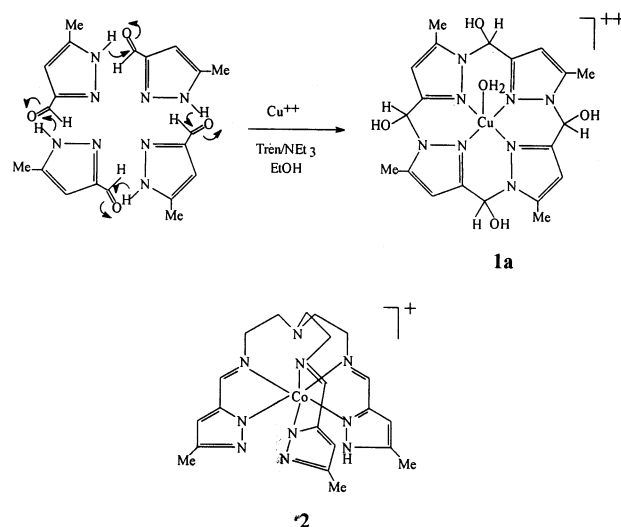


Figure 1. Plausible mechanism for macrocycle formation and structure of cation of the Co(III) tripodal complex.

formation, whereas it plays the pendant arm forming part of the tripodal ligand in the cases of Co(II) and Zn(II) ions. In this macrocycle formation, four pyrazole aldehyde units fuse together via aldol type condensation. We have also synthesized the macrocyclic complexes using equivalent amounts of another organic base, triethylamine (NEt₃).

Although various types of metal ion complexes with porphyrin or porphyrinogen-like macrocyclic ligands from pyrrole or other heterocycles^{1–8,25} have been synthesized and characterized, the macrocycle from pyrazole aldehyde is a new observation, and to the best of our knowledge, such type of macrocycle has not been reported until now. However, Bode et al.,²⁶ in a recent report, described the synthesis of a different type of macrocycle with built-in pyrazole groups and formation of its dinuclear Cu(II) complexes.

We have synthesized the Co(III) complex where the tripodal ligand formed in situ acts as a binategative N₆-donor system. We have also tried to synthesize the Co(III) complex in weakly alkaline media using 1 mmol/2 mmol organic base (NEt₃) and also in neutral medium. But interestingly, only one complex with same metal ligand stoichiometric ratio is obtained in all the cases. Ni(II) complexes of the same tripodal ligand have been synthesized, characterized and reported earlier.²⁷ The plausible mechanism for the macrocycle formation and both the structures of Cu(II) complex of the macrocyclic ligand and Co(III) complex of the tripodal one are given in Figure 1.

Experimental Section

Materials. Tren and DMSO were purchased from Aldrich. MPA was synthesized as described earlier.^{27,28} Spectrograde solvents were

- (6) (a) *Porphyryns and Metalloporphyryns*; Smith, K. M., Ed.; Elsevier: Amsterdam, 1975. *The Porphyrins*; Dolphin, D., Ed.; Academic: New York, 1978. (b) Mashiko, T.; Dolphin, D. In *Comprehensive Coordination Chemistry*; Wilkinson, G., Gillard, R. D., McCleverty, J. A., Eds.; Pergamon: Oxford, U.K., 1987; Vol. 2, Chapter 21.1, p 855. (c) Kim, J. B.; Adler, A. D.; Longo, R. F. In *The Porphyrins*; Dolphin, D., Ed.; Academic: New York, 1978; Vol. 1, Part A, p 85. Mauzerall, D. In *The Porphyrins*; Dolphin, D., Ed.; Academic: New York, 1978; Vol. 2, p 91. (d) Lindsey, J. S.; Schreiman, I. C.; Hsu, H. C.; Kearney, P. C.; Marguerettaz, A. M. *J. Org. Chem.* **1987**, *52*, 827. Lindsey, J. S.; Wagner, R. W. *J. Org. Chem.* **1989**, *54*, 828. (e) *Biosynthesis of Tetrapyrroles*; Jordan, P. M., Ed.; Elsevier: New York, 1991.
- (7) Bonomo, L.; Solari, E.; Scopelliti, R.; Floriani, C.; Re, N. *J. Am. Chem. Soc.* **2000**, *122*, 5312–5326.
- (8) (a) Pushpan, S. K.; Srinivasan, A.; Anand, V. G.; Venkatraman, S.; Chandrashekar, T. K.; Joshi, B. S.; Roy, R.; Furuta, H. *J. Am. Chem. Soc.* **2001**, *123*, 5138. (b) Pushpan, S. K.; Srinivasan, A.; Anand, V. G.; Chandrashekar, T. K.; Subramanian, A.; Roy, R.; Sugiura, K.-I.; Sakata, Y. *J. Org. Chem.* **2001**, *66*, 153.
- (9) Holm, R. H.; Kennepohl, P.; Solomon, P. I. *Chem. Rev.* **1996**, *96*, 2239–2314.
- (10) Karlin, K. D.; Zuberbühler, A. D. In *Bioinorganic Catalysis*, 2nd ed.; Reedijk, J., Bouman, E., Eds.; Marcel Dekker: New York, 1999; pp 469–534.
- (11) Fox, S.; Karlin, K. D. In *Active Oxygen in Biochemistry*; Valentine, J. S., Foote, C. S., Greenberg, A., Liebman, J. F., Eds.; Blackie Academic and Professional: Glasgow, Scotland, 1995; pp 188–231.
- (12) Kaim, W.; Rall, J. *Angew. Chem.* **1996**, *108*, 47–64.
- (13) Kitajima, N.; Moro-oka, Y. *Chem. Rev.* **1994**, *94*, 737–757.
- (14) Kitajima, N. *Adv. Inorg. Chem.* **1992**, *39*, 1–77.
- (15) *Bioinorganic Chemistry of Copper*; Karlin, K. D., Tycklar, Z., Eds.; Chapman & Hall: New York, 1993.
- (16) Orvig, C.; Berg, D. J.; Rettig, S. J. *J. Am. Chem. Soc.* **1991**, *113*, 2528.
- (17) Kirchner, R. M.; Mealli, C.; Bailey, M.; Howe, M.; Torre, L. P.; Wilson, L. J.; Andrews, L. C.; Rose, N. J.; Lingafelter, E. C. *Coord. Chem. Rev.* **1987**, *77*, 89.
- (18) Raghunathan, K. G.; Bharadwaj, P. K. *J. Chem. Soc., Dalton Trans.* **1992**, 2417.
- (19) Ghosh, P.; Shukla, R.; Chand, D. K.; Bharadwaj, P. K. *Tetrahedron* **1995**, *51*, 3265.
- (20) Sorrell, T. N.; Allen, W. E.; White, P. S. *Inorg. Chem.* **1995**, *34*, 952.
- (21) Mohamadou, A.; Gérard, C. *J. Chem. Soc., Dalton Trans.* **2001**, 3320.
- (22) Trofimenko, S. *Chem. Rev.* **1993**, *93*, 943.
- (23) Reviews of HC model system: (a) Sorrell, T. N. *Tetrahedron* **1989**, *45*, 3. (b) Karlin, K. D.; Tycklar, Z. *Adv. Inorg. Biochem.* **1994**, *9*, 120.
- (24) Abbreviations used: tren, tris(2-aminoethyl)amine; MPA, 5-methyl-3-formyl-pyrazole; TBAP, tetrabutylammonium perchlorate; DPPH, diphenylpicrylhydrazyl; TBP, trigonal bipyramid.

- (25) (a) Kalis, H. R.; Latos-Grazynski, L.; Balch, A. L. *J. Am. Chem. Soc.* **2000**, *122*, 12478. (b) Wolowicz, S.; Latos-Grazynski, L.; Mazzanti, M.; Marchon, J. C. *Inorg. Chem.* **1997**, *36*, 5761. (c) Chmielewski, P. J.; Latos-Grazynski, L. *Inorg. Chem.* **1997**, *36*, 840. (d) Chmielewski, P. J.; Latos-Grazynski, L. *Inorg. Chem.* **2000**, *39*, 5639.
- (26) Bode, R. H.; Bol, J. E.; Driessen, W. L.; Hulsbergen, F. B.; Reedijk, J.; Spek, A. L. *Inorg. Chem.* **1999**, *38*, 1239.
- (27) Paul, S.; Barik, A. K.; Butcher, R. J.; Kar, S. K. *Polyhedron* **2000**, *19*, 2661–2666.

Cu(II) Induced Formation of Porphyrinogen Derivative

used for physical measurements. All the other reagents and solvents were purchased from commercial sources and purified by standard procedures.

Syntheses. Warning! Perchlorate salts are potentially explosive and were handled only in small quantities with care.

Method A: [Cu(T₃-porphyrinogen)(H₂O)](NO₃)₂ (1a). A mixture of tren (0.146 g, 1 mmol) and MPA (0.33 g, 3 mmol) in EtOH (30 mL) was refluxed for 3 h. Then, the light yellow solution was cooled and filtered. To the filtrate was added Cu(NO₃)₂·6H₂O (0.30 g, 1 mmol), and the mixture refluxed again for ca. 2 h. The light green solution was then filtered and left in the air for slow evaporation at room temperature. A violet crystalline compound appeared after a week. It was filtered and washed with EtOH and dried in air (yield 40%). The product was recrystallized from hot EtOH. X-ray quality violet crystals were obtained by slow evaporation of the ethanolic solution of the complex at room temperature.

Method B. A mixture of MPA (0.44 g, 4 mmol) and NEt₃ (0.7 mL) was refluxed in absolute EtOH (30 mL) for ca. 3 h. To it was added Cu(NO₃)₂·6H₂O (0.30 g, 1 mmol), and the mixture refluxed again for 2 h. The light green solution was then filtered and kept for slow evaporation at room temperature. After a week, a violet crystalline compound was obtained. It was filtered and washed with EtOH and air-dried (yield 45%). Anal. Calcd for C₂₀H₂₆CuN₁₀O₁₁: C, 37.15; H, 4.02; N, 21.67. Found: C, 36.98; H, 4.14; N, 21.58. IR (KBr; cm⁻¹): 3365, 3228 (ν_{OH}), 1556 (w, C=NPz), 1387 (br, ν_{NO₃⁻}), 1069–1032 (ms, ν_{N-NPz}), 383 (ν_{Cu-O(H₂O)}), 254 (ν_{Cu-NPz ring}). Diffuse reflectance spectroscopy (DRS) (λ_{max}, nm): 566. UV-vis (MeOH, λ_{max}, nm (ε, M⁻¹ cm⁻¹)): 718 (69.9). UV-vis (DMF, λ_{max}, nm (ε, M⁻¹ cm⁻¹)): 787 (47). UV-vis (DMSO, λ_{max}, nm (ε, M⁻¹ cm⁻¹)): 854 (52) (broad). Molar conductivity (MeOH solution): Λ_m = 172 Ω⁻¹ cm² mol⁻¹. EPR (CH₃OH/C₂H₅OH) (77 K): g_{||} = 2.290, A_{||} = 160 G, g_⊥ = 2.067. Magnetism (solid state, room temperature): μ_{eff} = 1.70μ_B.}

[Cu(T₃-porphyrinogen)(H₂O)](ClO₄)₂ (1b). This compound was prepared following any one of the procedures described for 1a, except that Cu(ClO₄)₂·6H₂O was used as the metal ion precursor. Yield: 40% (Method A) and 45% (Method B). Anal. Calcd for C₂₀H₂₆Cl₂CuN₈O₁₃: C, 33.29; H, 3.60; N, 15.53. Found: C, 33.18; H, 3.76; N, 15.45. IR (KBr; cm⁻¹): 3362, 3220 (vb, ν_{OH}), 1558 (w, C=NPz), 1110 (br, ν_{ClO₄⁻}), 1065–1030 (ms, ν_{N-NPz}), 370 (ν_{Cu-O(H₂O)}), 262 (ν_{Cu-NPz ring}). DRS (λ_{max}, nm): 547. UV-vis (MeOH, λ_{max}, nm (ε, M⁻¹ cm⁻¹)): 721 (47.4) (broad). UV-vis (DMF, λ_{max}, nm (ε, M⁻¹ cm⁻¹)): 778 (47.4) (broad). UV-vis (DMSO, λ_{max}, nm (ε, M⁻¹ cm⁻¹)): 854 (51) (broad). Molar conductivity (MeOH solution): Λ_m = 204 Ω⁻¹ cm² mol⁻¹. Magnetism (solid state, room temperature): μ_{eff} = 1.63μ_B.}

[Co(HMPz₃tren)]ClO₄ (2). A mixture of tren (0.146 g, 1 mmol) and MPA (0.33 g, 3 mmol) in EtOH (30 mL) was refluxed for 2 h. The resulting light yellow solution was cooled and filtered. To the filtrate was added Co(ClO₄)₂·6H₂O (0.37 g, 1 mmol), and the mixture refluxed again for 2 h. The clear red solution obtained thereby was allowed to evaporate slowly. A red amorphous product was obtained after 7 days which was collected by filtration, washed with ethanol, and dried over fused CaCl₂ (yield 60%). The product was recrystallized from CH₃CN. X-ray quality crystals were grown by slow diffusion of benzene into CH₃CN solution of the compound. Anal. Calcd for C₂₁H₂₈ClCoN₁₀O₄: C, 43.53; H, 4.83; N, 24.18. Found: C, 43.41; H, 4.90; N, 24.03. IR (KBr; cm⁻¹): 3419, 3220 (vb, ν_{NH}), 1635 (s, ν_{C=N imine}), 1606 (s), 1581 (w, ν_{C-NPz}), 1091 (vb), 624 (s, ν_{ClO₄⁻}). DRS (λ_{max}, nm): 375, 485. UV-vis: no well-}

defined band in visible region. Molar conductivity (DMF solution): Λ_m = 89 Ω⁻¹ cm² mol⁻¹. ¹H NMR (d₆-DMSO, 300 MHz, 298 K): δ 2.20 (s, 9H, Me), 2.99 (m, 6H, N-CH₂), 3.17 (m, 6H, =N-CH₂), 6.64 (s, 3H, C₄-H-Pz), 8.26 (s, 3H, -N=C-H), 14.2 (s, 1H, Pz-NH).

[Zn(H₃MPz₃tren)](ClO₄)₂ (3). The compound was prepared by following method A, except that Zn(ClO₄)₂·6H₂O was used as the metal salt. Upon slow evaporation at room temperature, a sticky mass was obtained. It was dissolved in CH₃CN and purified on a silica gel column using 1:1 (v/v) benzene/acetonitrile mixture as eluant. The yellow fraction obtained was evaporated and solidified by scratching after addition of dry ether. Unfortunately, we were unable to grow X-ray quality crystals of this yellow microcrystalline compound. Anal. Calcd for C₂₁H₃₀Cl₂N₁₀ZnO₈: C, 36.7; H, 4.37; N, 20.39. Found: C, 37.08; H, 4.12; N, 20.55. ¹H NMR (d₆-DMSO, 300 MHz, 298 K): δ 2.27 (s, 9H, Me), 2.85 (m, 6H, N-CH₂), 3.13 (m, 6H, =N-CH₂), 6.61 (s, 3H, C₄-H-Pz), 8.55 (s, 3H, N=C-H), 13.0 (s, 3H, Pz-NH).

Physical Methods. UV-vis spectra were measured on a Hitachi U-3501 spectrophotometer. Infrared spectra were recorded on KBr disks (4000–200 cm⁻¹) with a JASCO FTIR model 420 spectrophotometer. ¹H NMR spectra were recorded with a Bruker AM300L (300 MHz) superconducting FT NMR. EPR spectra were obtained using a Varian E-112 spectrometer operating at X-band. The field was calibrated with a powder sample of DPPH (g = 2.0037). Solvents used were MeOH/EtOH (1:4 v/v) with copper complex concentration approximately 10⁻³ M. Room temperature magnetic moments were measured with a PAR 155 vibrating sample magnetometer. The diffuse reflectance spectra of the reported complexes were recorded on a Hitachi U-3501 spectrophotometer. Electrical conductivity measurements were carried out in MeOH or DMF solution using a Systronics model 304 digital conductivity meter. Elemental analyses were carried out at IACS, Calcutta, with a Perkin-Elmer model 2400 CHN analyzer. Cyclic voltammetry was carried out using Sycopel model AEW2 1820F/S instrument. The measurements were performed at 300 K in DMF solutions containing 0.2 M TBAP²⁴ and 10⁻³–10⁻⁴ M Cu(II) complex deoxygenated by bubbling with nitrogen. The working, counter, and reference electrodes used were a platinum wire, a platinum coil, and an SCE. Thermogravimetric analysis was carried out using Mettler Toledo model TGA/SDTA 851° instrument.

X-ray Crystal Structure Analysis. Relevant crystallographic data are collected in Table 1. Intensity data for the compounds were measured on an Enraf-Nonius CAD 4 diffractometer using graphite-monochromated Mo Kα radiation (λ = 0.71073 Å) in the ω-2θ scan mode. These were corrected for Lorentz-polarization effects. The structures were solved by using the SHELXS-97 package of programs and refined by full-matrix least-squares technique based on F² (SHELXL-97). Hydrogen atoms were added in the calculated positions.

Results and Discussion

The coordination compound of the expected tripodal ligand was synthesized in situ by template methodology in the presence of Co(II) and Zn(II) ions.

The ligand (H₃MPz₃tren) shows different extents of deprotonation in these complexes. In the cobalt(III) compound [Co(HMPz₃tren)]ClO₄ (2), it loses two protons, while, in the corresponding Zn(II) complex [Zn(H₃MPz₃tren)](ClO₄)₂ (3), it remains completely neutral. The same reaction when carried out with Cu(II) ion followed an unprecedented path, leading to porphyrinogen complexes (1a, 1b) involving the

(28) Barik, A. K.; Paul, S.; Kar, S. K.; Butcher, R. J.; Bryan, J. C. *Polyhedron* **1999**, *18*, 571.

Table 1. Crystal Data and Structure Refinement

	C ₂₀ H ₂₆ CuN ₁₀ O ₁₁	C ₂₀ H ₂₆ Cl ₂ CuN ₈ O ₁₃	C ₂₁ H ₂₈ ClCoN ₁₀ O ₄
fw	646.05	720.93	578.91
<i>T</i>	293(2) K	295(2) K	295(2) K
wavelength	0.71073 Å	0.71073 Å	0.71073 Å
cryst syst	monoclinic	monoclinic	monoclinic
space group	C2/c	C2/c	C2/c
unit cell dimensions	<i>a</i> = 19.476(3) Å	<i>a</i> = 20.967(3) Å	<i>a</i> = 21.293(3) Å
	<i>b</i> = 9.4116(8) Å	<i>b</i> = 9.1563(18) Å	<i>b</i> = 12.724(2) Å
	<i>c</i> = 14.204(3) Å	<i>c</i> = 14.858(4) Å	<i>c</i> = 19.777(4) Å
	α = 90°	α = 90°	α = 90°
	β = 107.58(2)°	β = 108.44(3)°	β = 93.03(2)°
	γ = 90°	γ = 90°	γ = 90°
<i>V</i> , <i>Z</i>	2482.0(7) Å ³ , 4	2706.0(10) Å ³ , 4	5350.6(15) Å ³ , 8
<i>D</i> (calcd)	1.729 mg/m ³	1.770 mg/m ³	1.437 mg/m ³
abs coeff	0.964 mm ⁻¹	1.088 mm ⁻¹	0.788 mm ⁻¹
<i>F</i> (000)	1332	1476	2400
cryst size	0.60 × 0.20 × 0.05 mm ³	0.40 × 0.20 × 0.10 mm ³	0.40 × 0.25 × 0.20 mm ³
θ range for data collection	2.19–25.00°	2.05–25.00°	1.87–25.00°
limiting indices	−23 ≤ <i>h</i> ≤ 22, 0 ≤ <i>k</i> ≤ 11, 0 ≤ <i>l</i> ≤ 16	−24 ≤ <i>h</i> ≤ 23, 0 ≤ <i>k</i> ≤ 10, 0 ≤ <i>l</i> ≤ 17	−25 ≤ <i>h</i> ≤ 25, 0 ≤ <i>k</i> ≤ 15, 0 ≤ <i>l</i> ≤ 23
reflns collected	2194	2385	4718
indep reflns	2194 (<i>R</i> _{int} = 0.0000)	2385 (<i>R</i> _{int} = 0.0000)	4716 (<i>R</i> _{int} = 0.0000)
completeness to θ = 25.00°	100%	100%	100%
abs correction	empirical used <i>ψ</i> -scans	empirical used <i>ψ</i> -scans	empirical used <i>ψ</i> -scans
max and min transm	0.6731 and 0.6252	0.8187 and 0.7322	0.8540 and 0.7914
refinement method	full-matrix least-squares on <i>F</i> ²	full-matrix least-squares on <i>F</i> ²	full-matrix least-squares on <i>F</i> ²
data/restraints/params	2194/0/197	2385/0/201	4718/0/334
GOF on <i>F</i> ²	1.034	1.045	1.017
final <i>R</i> indices [<i>I</i> > 2σ(<i>I</i>)]	<i>R</i> ₁ = 0.0414,	<i>R</i> ₁ = 0.0495,	<i>R</i> ₁ = 0.0545,
<i>R</i> indices (all data)	<i>wR</i> ₂ = 0.1119 <i>R</i> ₁ = 0.0656,	<i>wR</i> ₂ = 0.1424 <i>R</i> ₁ = 0.0830,	<i>wR</i> ₂ = 0.1892 <i>R</i> ₁ = 0.1033,
largest diff peak and hole	0.773 and −0.352 e Å ⁻³	0.659 and −0.403 e Å ⁻³	1.075 and −0.426 e Å ⁻³

pyrazole moiety as the building blocks. Despite our repeated attempts, we were unable to isolate the porphyrinogen molecule in the free state. When Cu(II) ion is removed from the porphyrinogen complexes (**1a** and **1b**) by sulfide precipitation, the product obtained is a pale yellow microcrystalline solid with a ¹H NMR spectrum [¹H NMR (*d*₆-DMSO, 300 MHz, 298 K): δ 2.18 (s, 3H, Me), 6.51 (s, C₄-H-Pz), 9.55 (s, 1H, CHO)] typical of the precursor aldehyde,²⁸ viz. MPA. The macrocycle formation fails to occur in the presence of other metal ions. The study of the TGA curve of complex **1a** confirms the loss of the coordinated water molecule in the temperature range 148–225 °C. The tripodal acts as N₆-binate for Co(III) complex because of the deprotonation of two N–H(Pz). The coordination polyhedron of the said complex is best described as distorted octahedral. The Co–N(10) distance (3.289 Å) shows that there is no bonding. The crystal structures of the Cu(II) complexes and the Co(III) complex are described in the following paragraphs.

Description of Crystal Structures: 1a and 1b. The ORTEP plot of the cationic portion of **1a** is represented in

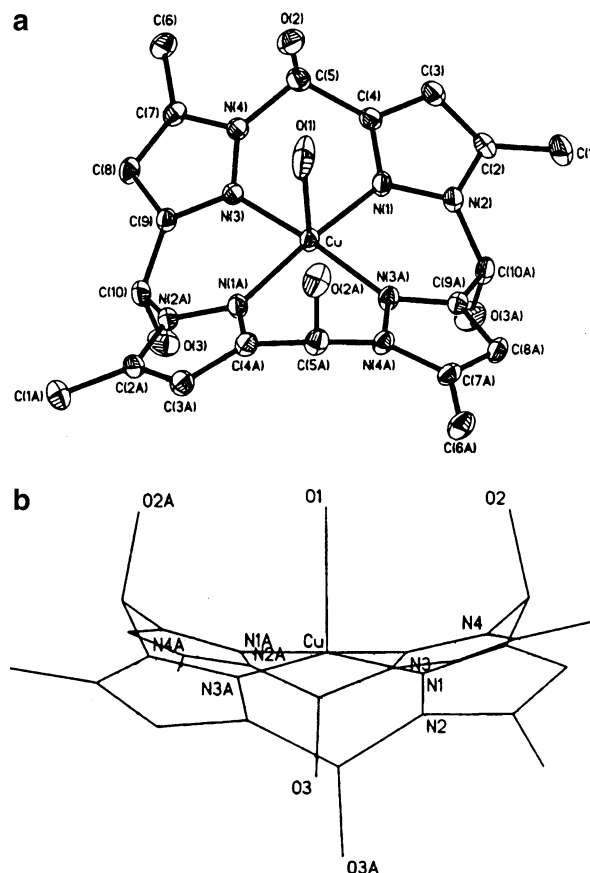


Figure 2. (a) ORTEP plot of the cation of **1a**. The thermal ellipsoids are drawn at the 30% probability level, and the hydrogen atoms are omitted for clarity. (b) Saddle distortion form of **1a**.

Table 2. Bond lengths (Å) and Angles (deg) for **1a** and **1b**

	1a	1b	
Bond Lengths			
Cu–N(1)#1	1.955(3)	Cu–N(1)#1	1.941(4)
Cu–N(3)#1	1.955(2)	Cu–N(3)#1	1.949(4)
Cu–O(1)	2.240(5)	Cu–O(1)	2.338(5)
Bond Angles			
N(1)#1–Cu–N(1)	171.40(18)	N(1)#1–Cu–N(1)	173.4(2)
N(1)–Cu–N(3)	89.33(22)	N(1)–Cu–N(3)#1	90.43(17)
N(1)–Cu–N(3)#1	89.89(12)	N(1)–Cu–N(3)	89.09(16)
N(1)#1–Cu–N(3)	89.89(12)	N(1)#1–Cu–N(3)#1	89.09(16)
N(1)#–Cu–N(3)#1	89.33(12)	N(1)#1–Cu–N(3)	90.43(17)
N(3)–Cu–N(3)#1	169.61(18)	N(3)#1–Cu–N(3)	171.6(2)
N(1)#1–Cu–O(1)	94.30(9)	N(1)#1–Cu–O(1)	93.28(11)
N(3)–Cu–O(1)	95.20(9)	N(3)#1–Cu–O(1)	94.19(11)
N(1)–Cu–O(1)	94.30(9)	N(1)–Cu–O(1)	93.28(11)
N(3)#1–Cu–O(1)	95.20(9)	N(3)–Cu–O(1)	94.19(11)

Figure 2a. Selected bond angles and distances of **1a** and **1b** are displayed in Table 2. The coordination geometry of the copper(II) atom in both the complexes reveals a distorted square pyramidal geometry. The geometry is completed by the oxygen atom of the water molecule in the apical site and four nitrogen donors from the unusual macrocyclic ligand occupying the basal plane. The Cu(II) atom is shifted approximately by 0.162 Å out of the basal plane for **1a** (0.126 Å for **1b**) toward the apical O atom. All the Cu–N bond distances are same in **1a** (1.955 Å) and almost same in **1b** (1.941 and 1.949 Å). These distances are shorter than similar bonds reported in other macrocyclic compounds^{26,29} and comparable with those reported for [Cu₂(N₆O)(OH)](BF₄)₂,

Cu(II) Induced Formation of Porphyrinogen Derivative

³⁰ [Cu(II)(pmea)Cl]ClO₄·H₂O,³¹ and [Cu(appn)](ClO₄)₂·H₂O (Cu₂Zn₂SOD model).³² The distortion induced in the presence of the pyrazole ring is reflected in the N(1)#1–Cu–N(1) and N(3)–Cu–N(3)#1 bond angles. These are 171.40(18)° and 169.61(18)° for **1a** (173.4(2)° and 171.6(2)° for **1b**), respectively.

The mean deviation of the basal plane N1A, N3, N1, and N3A is only 0.0151 Å (0.0156 Å for **1b**). The oxygen atom of the water molecule completes the coordination sphere by forming a bond to the metal at a distance of 2.240(5) Å [2.338(15) Å for **1b**]. In case of the perchlorate complex (**1b**), the Cu–O distance is within the range expected for an axially bound aquo molecule.^{32,33} This value is somewhat shorter in the case of the nitrate complex (**1a**), and this shorter value may be compared with a bond length of 2.263 Å obtained for the complex [CuL⁸] [H₂L⁸ = 1,4,8,11-tetraazacyclotetradecane-1,8-diacetic acid].³⁴ If the angle N(1)–Cu–O(1) is less than 80°, the coordinated O-atoms are laterally displaced from axial coordination sites.²⁹ In **1a**, the average angle value of 94.75(9)° [93.74(11)° for **1b**] strongly supports the axial coordination of the O-atom. The H₂O molecule of the axial coordination site is also H-bonded in both the complexes with their corresponding anions.

As the H-bond distance for the nitrate complex (2.665 Å) is shorter than that of the perchlorate complex (2.860 Å), a strong hydrogen bonding is indicated for the former and a moderate one for the latter.^{32,35}

Crystal structure studies show that the four OH groups present in the four chiral carbon atoms of T₃-porphyrinogen are in a trans disposition above and below the porphyrinogen mean plane. Interestingly, the pyrazole rings are situated downward with respect to the Cu atom. These observations reveal that the porphyrinogen ring is in a saddle-distorted form (Figure 2b).

Compound 2. An ORTEP plot of the cationic portion of **2** is presented in Figure 3. Selected metrical parameters are listed in Table 3. The potentially heptadentate H₃MPZ₃tren ligand coordinates to the Co(III) ion through the three imine and three pyrazole nitrogen atoms.

It is noteworthy that the bond angle C–N–C at N(10) is ca. 119° which is also in agreement with our previously determined value for the complex [Ni(H₃MPZ₃tren)](BF₄)₂·0.5H₂O.²⁷ The tertiary amine nitrogen atom N(10) appears to be the apex of a three-ribbed umbrella that has been inverted by the winds. Among different parameters, the height-to-bite ratio, *h/b*, is useful for describing the coordination polyhedra. An *h/b* ratio of 0.728 supports the octahedral geometry of the complex.¹⁷

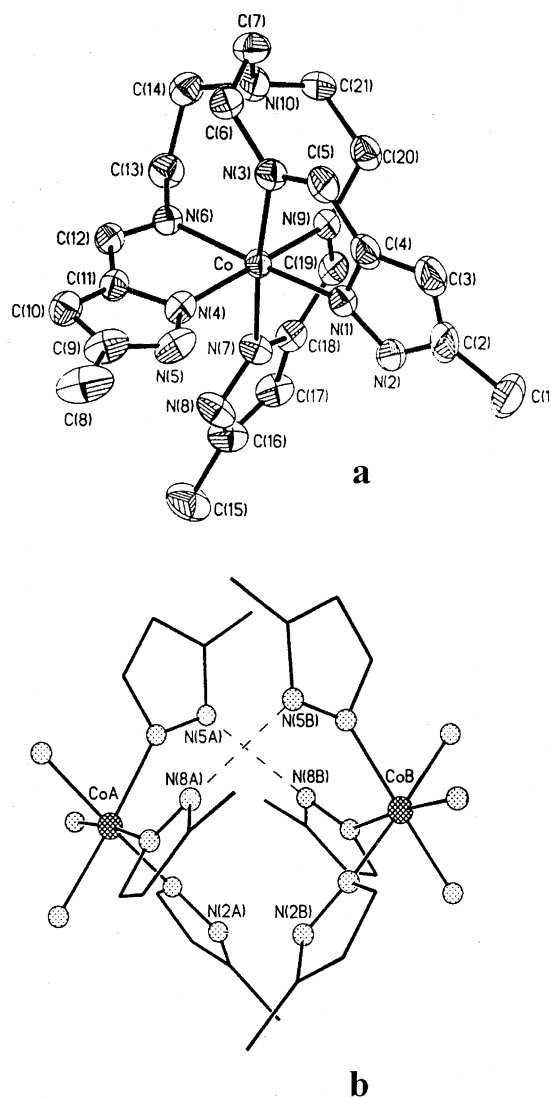


Figure 3. (a) ORTEP plot of the cation of **2**. The thermal ellipsoids are drawn at the 30% probability level, and the hydrogen atoms are omitted for clarity. (b) Hydrogen bonding mode of **2**.

Table 3. Selected Metrical Parameters for **2**

Bond Lengths		Bond Angles	
Co–N(4)	2.014(5)	N(4)–Co–N(7)	95.13(17)
Co–N(1)	2.016(5)	N(7)–Co–N(1)	97.08(19)
Co–N(7)	2.015(4)	N(7)–Co–N(9)	78.78(17)
Co–N(3)	2.055(5)	N(4)–Co–N(3)	88.86(17)
Co–N(9)	2.052(4)	N(1)–Co–N(3)	79.01(19)
Co–N(6)	2.055(4)	N(4)–Co–N(6)	78.75(17)
N(1)–N(2)	1.314(7)	N(1)–Co–N(6)	173.58(19)
N(4)–N(5)	1.350(6)	N(3)–Co–N(6)	95.83(17)
N(7)–N(8)	1.343(6)	N(4)–Co–N(1)	97.22(18)
		N(4)–Co–N(9)	171.97(17)
		N(1)–Co–N(9)	88.79(18)
		N(7)–Co–N(3)	174.75(18)
		N(9)–Co–N(3)	97.54(18)
		N(7)–Co–N(6)	88.30(17)
		N(9)–Co–N(6)	95.71(17)

From the Co–N bond distance values (Table 3), it is observed that the three Co–N(Pz) bond distances (average distance 2.015 Å) are shorter than Co–N(iminyl) bond distances (average distance 2.054 Å). This shortening of bond distance suggests that the N(pyrazolyl) atoms are the negative donor sites.

(29) Bernhardt, P. V.; Sharpe, P. C. *Inorg. Chem.* **2000**, *39*, 2020–2025.

(30) Sorrell, T. N.; Jameson, D. L.; O'Connor, C. J. *Inorg. Chem.* **1984**, *23*, 190.

(31) Schatz, M.; Becker, M.; Thaler, F.; Hampel, F.; Schindler, S.; Jacobson, R. R.; Tyekler, Z.; Murthy, N. N.; Ghosh, P.; Chen, Q.; Zubieta, J.; Karlin, K. D. *Inorg. Chem.* **2001**, *41*, 2312–2322.

(32) Liu, C.-M.; Xiong, R.-G.; You, X.-Z. *Polyhedron* **1997**, *16*, 119.

(33) Orpen, A. G.; Brammer, L.; Allen, F. H.; Kennard, O.; Watson, D. G.; Taylor, R. *J. Chem. Soc., Dalton Trans.* **1989**, 1.

(34) Chapman, J.; Ferguson, G.; Gallagher, J. F.; Jennings, M. C.; Parker, D. *J. Chem. Soc., Dalton Trans.* **1992**, 345.

(35) Cotton, F. A.; Wilkinson, G. *Advanced Inorganic Chemistry*, 5th ed.; Wiley: New York, 1988; p 93.

From the crystal packing diagram (Figure 3b), it is evident that the two Co units are linked together through H-bonding. As there is only one N–H(pyrazolyl) among the three uncoordinated N(pyrazolyl) (other two are deprotonated and satisfy the primary valency of Co(III) ion), there are two H-bonding possibilities. Figure 3b shows both the H-bondings, CoAN(5A)⋯N(8B)CoB and CoAN(8A)⋯N(5B)CoB. Both the distances are of same value (2.777 Å) indicating moderately strong H-bonding.^{32,35}

Diffuse Reflectance and Solution Spectra. The diffuse reflectance spectra of the Cu-complexes exhibit only one broad band around 566 nm for **1a** and 547 nm for **1b** indicating the square pyramidal geometry of the complex species. Similar observations with a little deviation in band position are also reported for the same chromophore CuN₄O where N-donor sites are from pyrazole rings^{13,36,37} and also for single-crystal spectra of chelate complex [Cu(1,3-Pn)₂·H₂O]SO₄.³⁸ Probably, the macrocyclic ring effect may be responsible for creating such deviation. In MeOH solution, the complexes display absorption bands at 718 nm ($\epsilon = 69.9 \text{ M}^{-1} \text{ cm}^{-1}$) and 721 nm ($\epsilon = 47.4 \text{ M}^{-1} \text{ cm}^{-1}$) for **1a** and **1b**, respectively. This corresponds to d–d transition of Cu(II) in a weak tetragonal field and is in accordance with those reported for SOD mimicking compounds.^{32,39–41} This shift in λ_{max} value in solution from that of the solid state may be due to replacement of the weakly coordinated H₂O molecule in the fifth position by the solvent molecule maintaining the same geometry.³⁷ This proposition is further substantiated from the EPR spectrum of the complex (discussed later). Interestingly, when the spectra are recorded in DMF solution, the λ_{max} is shifted toward higher wavelengths. This trend is also followed in DMSO solvent and to a much greater extent. The red shift in optical spectra may be attributed to the strong coordinating property of the solvent, which results in the lowering in energy gap between two spin states. Nonplanarity is known to cause a red shift in the optical spectra of porphyrins due to greater destabilization of the HOMO compared with the LUMO.⁴² In strongly coordinating solvents, the original nonplanarity of the CuN₄ chromophore is further enhanced because of the formation of a stronger bond with the solvents at the apical position.

The diffuse reflectance spectrum of the Co-complex exhibiting two bands at 375 nm ($^1A_{1g} \rightarrow ^1T_{1g}$) and at 485 nm ($^1A_{1g} \rightarrow ^1T_{2g}$) indicates the low spin octahedral geometry of the [Co(HMPz₃tren)]⁺ cation. Probably, the other bands are masked by the intense charge-transfer bands in UV region. That in DMF solution the complex exhibits no band in the visible region may be due to intrusion of tails of intense

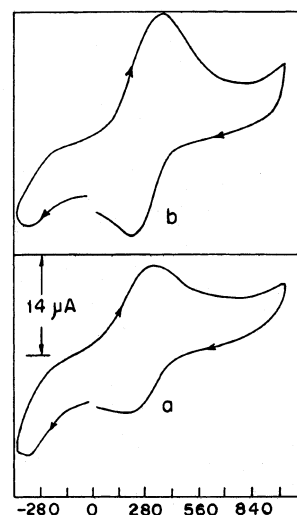


Figure 4. Cyclic voltammograms of **1a**: (a) 100 mV s⁻¹, (b) 250 mV s⁻¹. All potentials are given versus SCE. All measurements have been carried out in 0.2 M TBAP/DMF at 300 K.

charge-transfer bands into the visible portion of the spectrum, which masks the expected d–d bands.⁴³

EPR Spectroscopy. It is known that the EPR spectral pattern for square pyramidal complexes of Cu(II) ($d_{x^2-y^2}$ ground state (gs)) is quite different from that observed for TBP²⁴ (d_{z^2} gs). In general, frozen solution EPR spectra of square pyramidal complexes are characterized by an axial pattern with the features $g_{\parallel} > 2.1 > g_{\perp} > 2.0$ and $|A_{\parallel}| = 120\text{--}150 \times 10^{-4} \text{ cm}^{-1}$.^{44–48} whereas complexes with the TBP structure typically show EPR spectra having a “reversed axial” appearance with $g_{\perp} > g_{\parallel} \approx 2.0$ and $|A_{\parallel}| = (60\text{--}100) \times 10^{-4} \text{ cm}^{-1}$.^{44,46–48} Thus, the coordination geometry around the central metal ion in the Cu-complex can be deduced from an examination of the EPR spectral features. The EPR spectrum of **1a** has been recorded in frozen solution (MeOH/EtOH, 1:4 v/v) at 77 K (X-band frequency). The spin-Hamiltonian parameters g_{\parallel} (2.290) $> 2.1 > g_{\perp}$ (2.067) > 2.0 and $A_{\parallel} = 160 \times 10^{-4} \text{ cm}^{-1}$ are typical of a square pyramidal geometry in solution.³¹ Here, the value $G > 4.0$ indicates that the local tetragonal axes are aligned parallel or only slightly misaligned.³⁸

Electrochemistry. The electron-transfer behavior of the Cu(II) complexes (**1a** and **1b**) are grossly identical as revealed by cyclic voltammetry. A representative voltammogram for **1a** in DMF is shown in Figure 4. It involves a quasireversible one-electron process at $E_{1/2} = 0.260 \text{ V}$ (0.262 V for **1b**) versus SCE (scan rate 100 mV/s). A comparison with the Fe/Fe⁺ couple indicates the involvement of a single electron in this redox process.⁴⁹ We believe this process to

(36) Lever, A. B. P. *Inorganic Electronic Spectroscopy*; Elsevier: New York, 1984; pp 560–570.

(37) Deters, R.; Krämer, R. *Inorg. Chem. Acta* **1998**, 269, 117–124.

(38) Hathaway, B. J.; Billing, D. E. *Coord. Chem. Rev.* **1970**, 5, 143–207.

(39) Long, L.-S.; Tong, Y.-X.; Yang, S.-P.; Chen, X.-M.; Ji, L.-N. *Transition Met. Chem. (London)* **1999**, 24, 440–444.

(40) Lu, Q.; Shin, C.-Y.; Luo, Q.-H. *Polyhedron* **1993**, 12, 2005.

(41) Luo, Q.; Lu, Q.; Dai, A.; Huang, L. *J. Inorg. Biochem.* **1993**, 51, 655.

(42) Shelnutz, J. A.; Song, X.-Z.; Ma, J.-G.; Jia, S.-L.; Jentzen, W.; Medforth, C. *Chem. Soc. Rev.* **1998**, 27, 31 and references therein.

(43) Barik, A. K.; Paul, S.; Butcher, R. J.; Kar, S. K. *Polyhedron* **2000**, 19, 2651.

(44) Addison, A. W.; Hendriks, H. M. J.; Reedijk, J.; Thompson, L. K. *Inorg. Chem.* **1981**, 20, 103–110.

(45) Duggan, M.; Ray, N.; Hathaway, B.; Tomlinson, G.; Briant, P.; Plein, K. *J. Chem. Soc., Dalton Trans.* **1980**, 1342–1348.

(46) Nishida, Y.; Oishi, N.; Kida, S. *Inorg. Chim. Acta* **1980**, 44, L257–L258.

(47) Takahashi, K.; Ogawa, E.; Oishi, N.; Kida, S. *Inorg. Chim. Acta* **1982**, 66, 97–103.

(48) Morpurgo, L.; Falcioni, R.; Rotildo, G.; Desideri, A.; Mondovi, B. *Inorg. Chim. Acta* **1978**, 28, L141–L143.

Cu(II) Induced Formation of Porphyrinogen Derivative

be due either to a Cu(II)/Cu(III) electron transfer or a ligand-based process. Coulometric confirmation of electron stoichiometry was vitiated by the slow decomposition of these molecules in the time scale of this measurement.

Conclusion and Comments

Using the same synthetic procedure, we have synthesized two different ligands: one of which is an unsaturated macrocycle, and the other is a tripodal. Tren acts as a base for macrocycle formation and the pendent arm for the tripodal ligand. Ni(II),²⁷ Zn(II), and Co(III) metal ions do not form macrocycles. The macrocycle formation is unique for Cu(II). The plasticity of copper geometry probably can withstand the strain imposed by the saddlelike arrangement of this novel pyrazole-based macrocycle. In the Co(III) complex, the ligand is binegative, and only one type of complex

is formed at different pHs whereas, in the cases of Ni(II) and Zn(II), the ligand acts as a neutral one.

Acknowledgment. Acknowledgment is made to the University Grants Commission, New Delhi, India, for awarding a minor research project in science [PSW-063/00-01(ERO)] to S. Paul. We thank Prof. K. Nag, Prof. Muktimoy Chaudhury of IACS, and Dr. K. Pramanik of Jogomaya Devi College, Calcutta, for many discussions.

Supporting Information Available: Crystallographic data in CIF format. This material is available free of charge via the Internet at <http://pubs.acs.org>.

IC0112185

(49) Gagné, R. R.; Koval, C. A.; Lisensky, G. C. *Inorg. Chem.* **1980**, *19*, 2584.